Isochronal synchronization of delay-coupled systems

Ira B. Schwartz and Leah B. Shaw
U.S. Naval Research Laboratory, Code 6792, Nonlinear Systems Dynamics Section, Plasma Physics Division, Washington, DC 20375, USA

(Received 9 September 2006; revised manuscript received 21 February 2007; published 12 April 2007)

We consider small network models for mutually delay-coupled systems which typically do not exhibit stable isochronally synchronized solutions. We show analytically and numerically that for certain coupling architectures which involve delayed self-feedback to the nodes, the oscillators become isochronally synchronized. Applications are shown for both incoherent pump-coupled lasers and spatiotemporal coupled fiber ring lasers.

DOI: 10.1103/PhysRevE.75.046207 PACS number(s): 05.45.Xt, 42.65.Sf, 42.55.Wd

Synchronization of networked, or coupled, systems has been examined for large networks of identical [1] and heterogeneous oscillators [2]. For coupled systems with smaller numbers of oscillators, several new dynamical phenomena have been observed, including generalized [3], phase [4], and lag [5] synchronization. Lag synchronization, in which there is a phase shift between observed signals, is one of the routes to complete synchrony as coupling is increased [5] and may occur without the presence of delay in the coupling terms.

For systems with delayed coupling, a time lag between the oscillators is typically observed, with a leading time series followed by a lagging one. Such lagged systems are said to exhibit achronal synchronization. In [6], the existence of achronal synchronization in a mutually delay-coupled semiconductor laser system was shown experimentally and, in [7], studied theoretically in a single-mode semiconductor laser model. In the case of short coupling delay for unidirectionally coupled systems, anticipatory synchronization occurs when a response in a system's state is not replicated simultaneously but instead is anticipated by the response system [8,9], and an example of anticipation in synchronization is found in coupled semiconductor lasers [10]. Cross-correlation statistics between the two intensities showed clear maxima at delay times consisting of the difference between the feedback and the coupling delay. Anticipatory responses in the presence of stochastic effects have been observed in models of excitable media [11], as well as in experiments of coupled semiconductor lasers in a transmitter-receiver configuration [12]. When the zero-lag state is unstable and achronal synchronization occurs, the situation may be further complicated by switching between leader and follower. Switching has been observed theoretically and experimentally in stochastic systems [13] but may occur even in deterministic chaotic systems [14].

Given that both lag and anticipatory dynamics may be observed in delay-coupled systems, it is natural to ask whether the isochronal, or zero-lag, state, in which there is no phase difference in the synchronized time series, may be stabilized in coupled systems. Understanding isochronal synchrony in delay-coupled systems is important in many fields where long-range correlations play a role in network architecture. Evidence of long-range correlations leading to synchronized clusters has appeared in the visual cortex [15] and dynamical cortical neurons [16]. Additional feedback loops have been used in simple models incorporating long-range correlations of neurons to enhance synchrony as well [17]. Stabilizing the isochronal state is very important in bidirectional chaotic communication systems, as shown in recent theoretical work on communicating in systems with delay [18].

Stable isochronal synchronization of semiconductor lasers has been observed recently in experiments [19,20] and numerically [20,21]. Examples of partial isochronal synchrony, in which only some of the oscillators in a delay network synchronize, may be found in [18,22], and recently a theoretical explanation for partial synchronization has appeared in [23]. Other examples of isochronal synchrony have appeared in neural network models with delay [24,25].

In this paper, we explore the possibility of adding self-feedback to two globally coupled situations: (i) Incoherent delay-coupled semiconductor systems [26] and (ii) coupled spatiotemporal systems consisting of coupled fiber ring lasers [27] with delay [28].

We consider N coupled oscillators of the following form. Let F denote an m-dimensional vector field, B an $m\times m$ matrix, and κ_j, where $j=1,\ldots,N$, denote the coupling constants. For the cases we examine here, we consider global coupling including self-feedback:

$$\frac{dx_i(t)}{dt}=F(x_i(t),x_i(t-\tau))+\sum \kappa_j B x_j(t-\tau), \quad j\neq i. \quad (1)$$

Given the structure of Eq. (1), we examine the stability transverse to the synchronized state, $S=\{x_i(t):x_i(t)=s(t),\ i=1,\ldots,N\}$, by defining $\eta_{ij}\equiv x_j-x_i$. The linearized variations in the direction transverse to S are then given by

$$\frac{d\eta_{ij}(t)}{dt}=D_1F(x_i(t),x_i(t-\tau))\,\eta_{ij}(t)+D_2F(x_i(t),x_i(t-\tau))\times\eta_{ij}(t-\tau)+(\kappa_i-\kappa_j)Bx_i(t-\tau)-\kappa_j B\,\eta_{ij}(t-\tau), \quad (2)$$

where D_i denotes the partial derivative with respect to the ith argument.

We make the following hypotheses to simplify the analysis: (H1) Assume that the dependence on the time delayed variables in F takes the same form as the delay coupling; i.e., $D_2F(x,y)=B\kappa_f$. (H2) Let $\kappa_i=\kappa_f=\kappa$, $i=1,\ldots,N$. Equation (2) then simplifies to

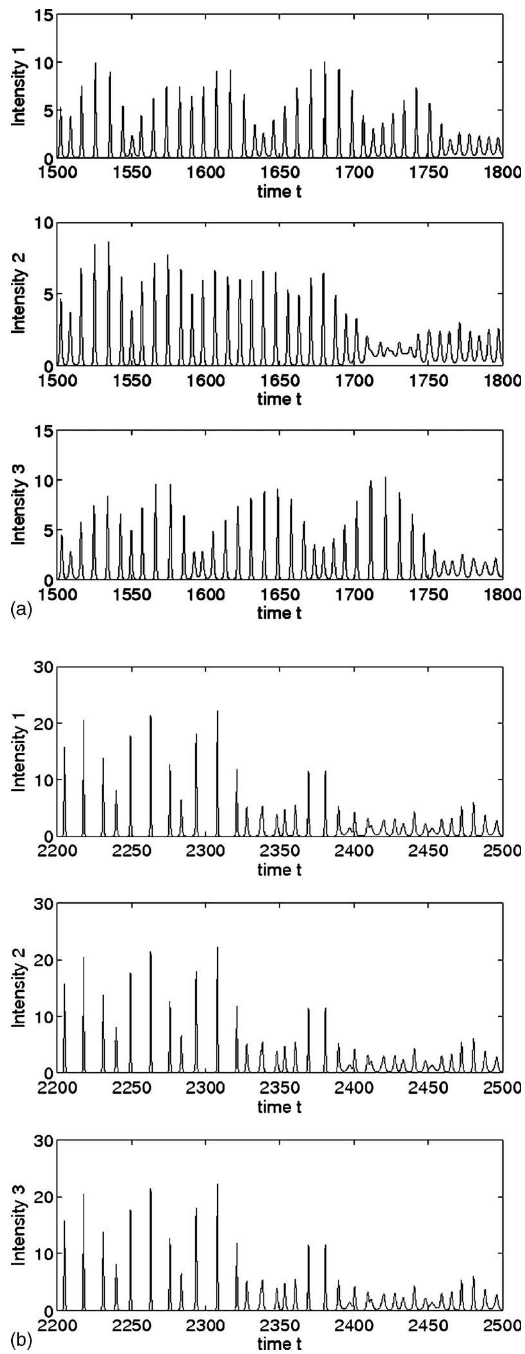

FIG. 1. An example of delay-coupled dynamics showing intensities computed for $N=3$, $\kappa=3.0\epsilon$, $\tau=30$, $a=2$, $b=1$, and $\epsilon=\sqrt{0.001}$, using Eq. (4). (a) shows a solution where the lasers are coupled globally without self-feedback, in which isochronal synchrony does not occur. (b) shows a stable isochronal solution with self-feedback terms included.

$$\frac{d\eta_{ij}(t)}{dt} = D_1F(x_i(t),x_i(t-\tau))\,\eta_{ij}(t), \tag{3}$$

where it is understood that the arguments of the derivatives are computed along the synchronized solution $s(t)$ and the solution is a function of parameters such as coupling and delay. Computing Eq. (3) along the synchronized state will generate the Lyapunov exponents for the transverse directions, and we examine the effect of coupling and delay by computing the cross correlations between time series as well.

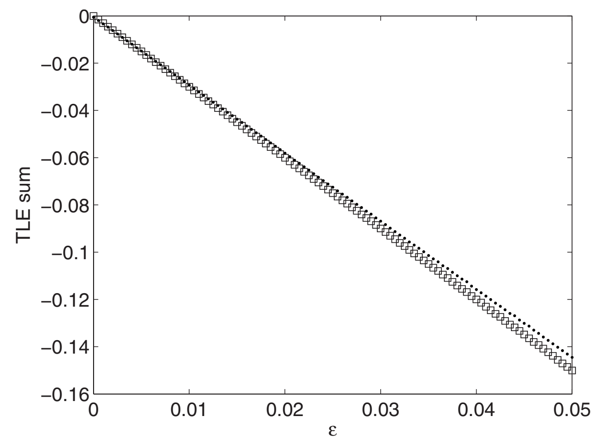

FIG. 2. Prediction of the scaling of the sum of transverse Lyapunov exponents for Eq. (5) with respect to ϵ. Other parameter values are as in Fig. 1(b). Squares are the prediction using Eq. (7), and dots are the numerical values.

To examine the stability of the isochronally synchronized state of Eq. (1), we model $N=3$ lasers that are pump coupled [26,29]. An isolated semiconductor laser's dynamics at the ith node is governed by $\frac{dz_i}{dt}=\bar{F}(z_i)$, $z_i=(x_i,y_i)$, where

$$\bar{F}(z) = (-y - \epsilon x(a+by), x(1+y)), \tag{4}$$

and x and y are the scaled carrier fluctuation number and normalized intensity fluctuations about steady state zero, respectively. ϵ^2 is the ratio of photon to carrier lifetimes, and a and b are dimensionless constants (see [30] for details on the derivation).

The coupling strengths are $\kappa_i=\kappa_f=\kappa$, $i=1,2,3$. This leads to the following set of differential equations for the system:

$$\frac{dz_i(t)}{dt} = \bar{F}(z_i(t)) + \kappa\sum_{i=1}^{3} Bz_i(t-\tau), \quad i=1,2,3, \tag{5}$$

where $m=2$ and $B(1,2)=1$, with all other entries in B equal to 0. An example of the intensities with and without self-feedback in Fig. 1 shows explicitly the effect of self-feedback in stabilizing the isochronal solution. Writing down the differential equation for the transverse directions in matrix form for Eq. (5) using Eq. (3) and expanding near the synchronized solution $\eta_{ij}=0$, we obtain $X'(t)=A(t,\kappa,\tau,\epsilon)X(t)$, where $A(t,\kappa,\tau,\epsilon)=DF(s(t,\kappa,\tau,\epsilon))$ and $X(0)=I$. Due to the nature of the global coupling with self-feedback, each node receives the same signal. Therefore, the transverse stability does not explicitly depend on the coupling or delay, but rather on the dynamics of local nodes [31]. To examine the stability of the isochronal state, we derive some properties of the transverse Lyapunov exponents (TLEs). The TLEs satisfy the following limit: $\lambda(x_0,y_0,u)=\lim_{t\to\infty}\frac{1}{t}\ln\frac{\|X(t)u\|}{\|u\|}$. Here u is a vector in a given direction.

By computing the solution to the linear variational equations along a given solution, we can extract the TLEs. To

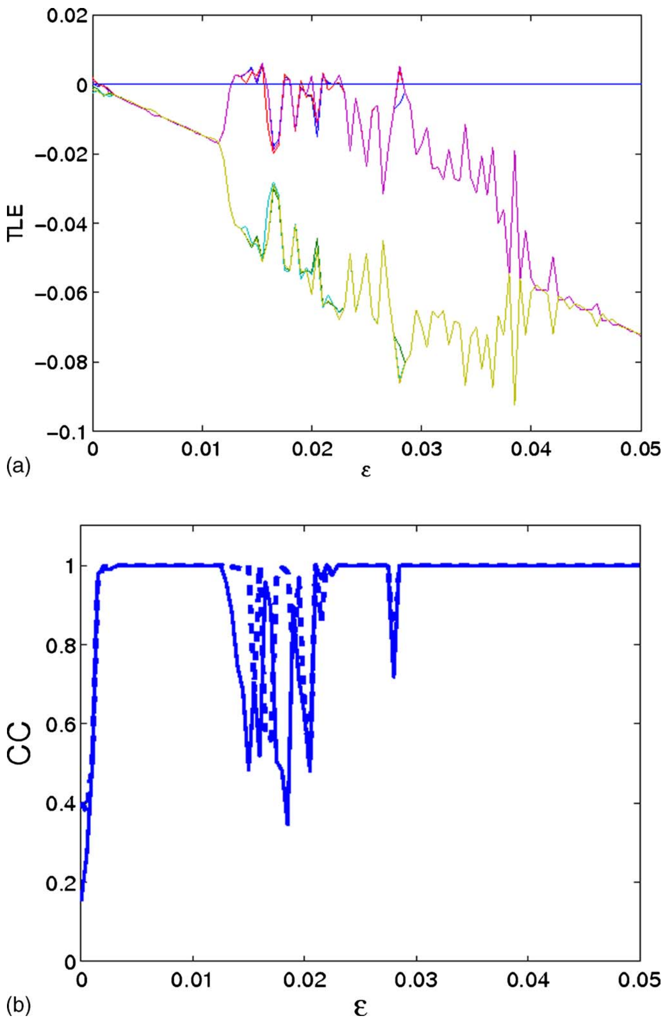

FIG. 3. (Color online) (a) All transverse Lyapunov exponents and (b) cross correlation (CC) of the dynamics for the same conditions as in Fig. 2. In (b), the cross correlations between lasers 1 and 2 (solid line) and 1 and 3 (dashed line) are shown. For most values of ϵ shown here, a cross correlation of 1 is achieved when the shift between the time traces is zero, showing that the isochronal solution is stable.

examine the scaling behavior of the TLEs, let $\Delta(t,\kappa,\tau,\epsilon) = \det[X(t,\kappa,\tau,\epsilon)]$. Then, we have that $\Delta(t,\kappa,\tau,\epsilon) = \exp\{\int_0^t \mathrm{tr}[A(s,\kappa,\tau,\epsilon)]ds\}$ [32]. Taking the logarithm of the matrix solution and noting that the determinant of a matrix is the product of its eigenvalues, we have

$$\sum_{i=1}^{m} \lambda(x_0,y_0,e_i) = \lim_{t\to\infty} \frac{1}{t} \ln|\det[X(t,\kappa,\tau,\epsilon)]|, \qquad (6)$$

where e_i are arbitrary independent basis vectors. Equation (6) yields a rate of volume change in the dynamics in the transverse directions. The solution may still be chaotic with one or more exponents being positive, but if sufficiently dissipative, volumes will shrink over time.

From Eq. (4), since $\mathrm{tr}[A(t,\kappa,\tau,\epsilon)] = -\epsilon[a + by(t,\kappa,\tau,\epsilon)] + x(t,\kappa,\tau,\epsilon)$ and assuming that the inversion $x(t,\kappa,\tau,\epsilon)$ has zero time average due to symmetry (which is observed numerically [34]), we have $\int_0^t \mathrm{tr}[A(s,\kappa,\tau,\epsilon)]ds = -\epsilon(a + b\langle y_{\kappa,\tau,\epsilon}\rangle)t$, and from Eq. (6), we have

$$\lambda(x_0,y_0,e_1) + \lambda(x_0,y_0,e_2) = -\epsilon(a + b\langle y_{\kappa,\tau,\epsilon}\rangle). \qquad (7)$$

Since ϵ appears explicitly, it is easy to see how the sum of the TLEs scales with ϵ and compares with numerical experiments as in Fig. 2.

Although the sum of the TLE is negative, loss of synchrony due to instability may occur at intermediate values of ϵ, as seen in Fig. 3. Regions where the isochronally synchronized solution is unstable are associated with one or more positive transverse Lyapunov exponenents. On the other hand, for sufficiently large damping, the transverse exponents reveal a stronger overall reduction in the phase-space volume. The stability of isochronal synchrony with respect to other parameters can also be computed, e.g., as shown in Fig. 4 for variations in coupling strength κ.

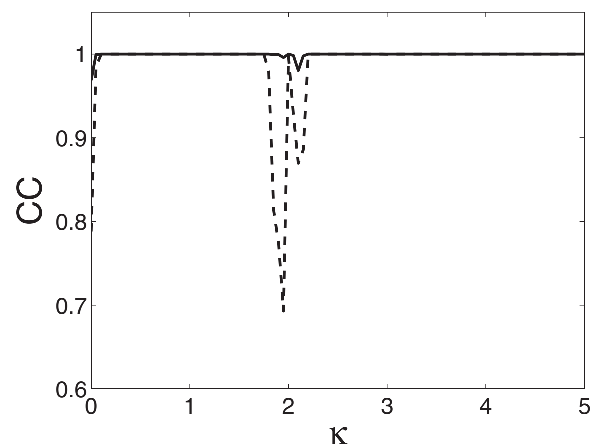

FIG. 4. Cross correlation (CC) between lasers 1 and 2 (solid line) and between 1 and 3 (dashed line) vs coupling κ for Eq. (5). Other parameters are the same as in Fig. 1(b).

To illustrate the robustness of the self-feedback structure for generating isochronal synchronization in delay-coupled systems, we examine a spatiotemporal stochastic system with multiple delays composed of coupled fiber ring lasers. A fiber ring laser system without self-feedback was studied in [28], and we extend the same model to include self-feedback terms. In each ring laser, light circulates through a ring of optical fiber, at least part of which is doped for stimulated emission. The time for light to circulate through the ring is the cavity round-trip time $\tau_R = 202$ ns, and the delay time in the coupling and self-feedback lines is a second delay $\tau_d = 45$ ns. Each laser is characterized by a total population inversion $W(t)$ and an electric field $E(t)$. The equations for the model dynamics of the jth laser are as follows:

$$E_j(t) = R\exp[\Gamma(1 - i\alpha_j)W_j(t) + i\Delta\phi]E_j^{\mathrm{fdb}}(t) + \xi_j(t), \qquad (8)$$

$$\frac{dW_j}{dt} = q - 1 - W_j(t) - |E_j^{\mathrm{fdb}}(t)|^2\{\exp[2\Gamma W_j(t)] - 1\}. \qquad (9)$$

The electric field from earlier times which affects the field at time t is

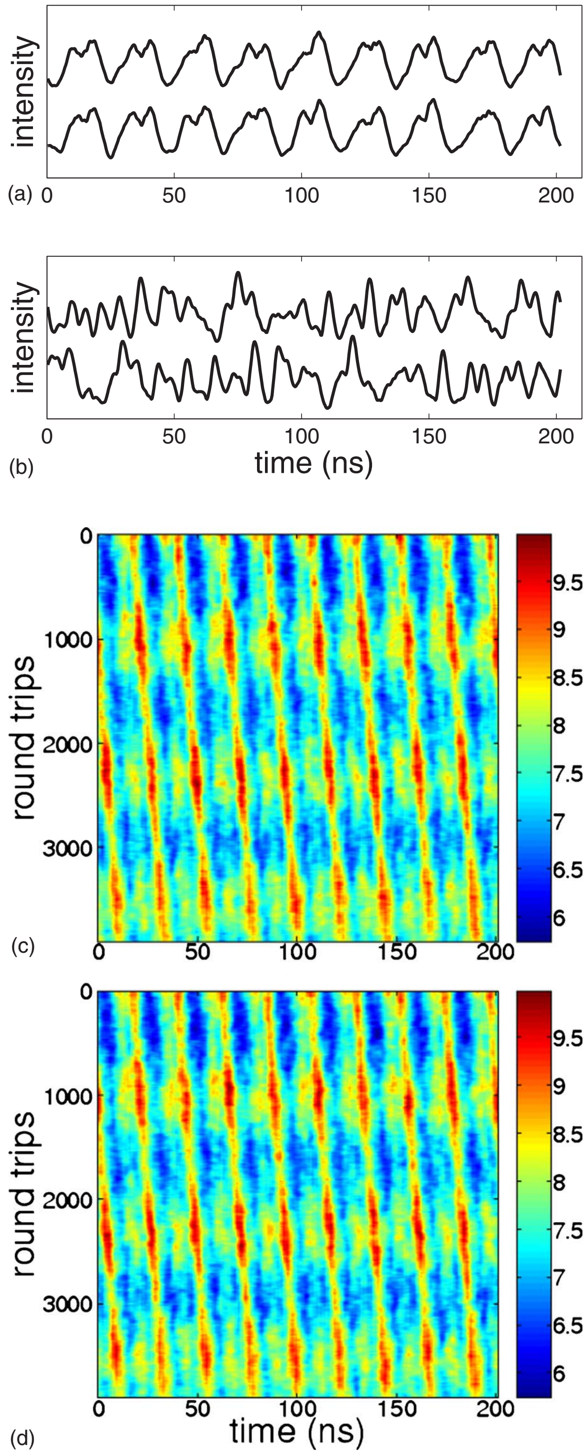

FIG. 5. (Color online) Intensity (arbitrary units) for two lasers coupled with $\kappa=0.009$. The left panels are intensity vs time for laser 1 (bottom curve) and for laser 2 (top curve): (a) with self-feedback and (b) without self-feedback. Spatiotemporal plots corresponding to coupling with self-feedback for (c) laser 1 and (d) laser 2.

$$E_j^{\text{fdb}}(t) = E_j(t-\tau_R) + \sum_{l\neq j} \kappa_l E_l(t-\tau_d) + \kappa_f E_j(t-\tau_d). \quad (10)$$

$E_j(t)$ is the complex envelope of the electric field in laser j, measured at a given reference point inside the cavity. $E_j^{\text{fbd}}(t)$ is a feedback term that includes optical feedback within laser j and optical coupling with the other laser. Time is dimensionless. Energy input is given by the pump parameter q. Each electric field is perturbed by independent complex Gaussian noise sources ξ_j, with standard deviation D. We use a fixed input strength for all coupling terms: $\kappa_i=\kappa_f=\kappa$ for all i. (Values of the parameters in the model as well as further computational details can be found in [28]. The only difference in parameters is that the lasers are not detuned relative to each other in the current work.)

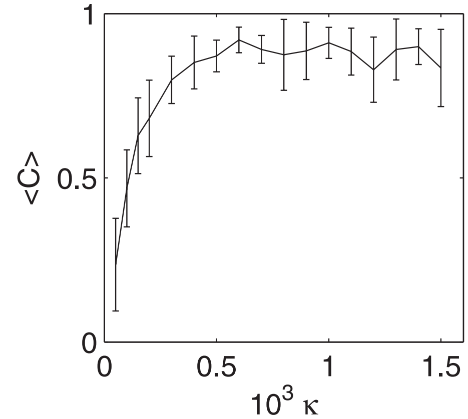

FIG. 6. Average cross correlation vs coupling for two coupled lasers with self-feedback.

Because of the feedback term $E_j^{\text{fdb}}(t)$ in Eq. (8), one can think of Eq. (8) as mapping the electric field on the time interval $[t-\tau_R, t]$ to the time interval $[t, t+\tau_R]$ in the absence of coupling ($\kappa=0$). Equivalently, because the light is traveling around the cavity, Eq. (8) maps the electric field at all points in the ring at time t to the electric field at all points in the ring at time $t+\tau_R$. We can thus construct spatiotemporal plots for $E(t)$ or the intensity $I(t)=|E(t)|^2$ by unwrapping $E(t)$ into segments of length τ_R.

Figure 5 shows time traces of the $N=2$ lasers for a single round trip for both the system with self-feedback described here and the system without self-feedback ($\kappa_f=0$) [33]. Isochronal synchrony can been seen when self-feedback is included, while in the absence of self-feedback the lasers are delay synchronized. The spatiotemporal plots in Figs. 5(c) and 5(d) are nearly identical due to the isochronal synchrony. To quantify the synchrony, we align the time traces for the two lasers with various time shifts between them. In the absence of self-feedback, the peak cross correlation occurs when the lasers are shifted relative to each other by the delay time. The cross correlation is low when the lasers are compared with no time shift. In contrast, when self-feedback is included, the lasers achieve a high degree of correlation when compared isochronally. For the time traces shown in Fig. 5(a), the peak cross correlation of 0.9554 occurs when there is no time shift, although the cross correlation when shifted by the delay time is nearly as high (0.9549).

We have swept the coupling strength κ for the system of two lasers with self-feedback and computed the average cross correlation when the lasers are compared isochronally. Figure 6 shows that the lasers are well synchronized for input strengths as small as 0.1%. Isochronal synchronization can be produced when the lasers are detuned as in [28], but this requires stronger coupling and self-feedback (not shown).

For $N=3$ fiber ring lasers, we have done a similar computation for cases with and without self-feedback (not shown). We found that when the the lasers are coupled globally without self-feedback, the isochronal state will still synchronize. However, adding self-feedback will cause the isochronal state to stabilize at somewhat lower values of coupling. Further details for this case are in [34].

In summary, we have considered delay-coupled systems and, through the addition of self-feedback, obtained stable isochronal synchrony in coupled semiconductor and fiber ring laser models. Model analysis for incoherent pump coupled lasers reveals scaling of the Lyapunov exponents transverse to the synchronized state, while computations on systems of coupled fiber ring lasers show how self-feedback may cause the onset of synchrony in coupled spatiotemporal systems. In the cases we have studied, we constructed small globally coupled networks. For the small clusters presented here with delay, it is advantageous to add feedback loops, since this was key to stabilizing the synchronous state. A question for future study is how this method may be scaled up for larger networks.

The authors thank Alexandra Landsman, Rajarshi Roy, and Anthony Franz for very stimulating discussions and comments. L.B.S. is currently a National Research Council Post Doctoral fellow. The authors also acknowledge the support of the Office of Naval Research.

[1] A. Pikovsky, M. Rosenblum, and J. Kurths, *Synchronization: A Universal Concept in Nonlinear Science* (Cambridge University Press, Cambridge, England, 2001).
[2] J. G. Restrepo, E. Ott, and B. R. Hunt, Phys. Rev. Lett. **96**, 254103 (2006).
[3] N. F. Rulkov, M. M. Sushchik, L. S. Tsimring, and H. D. I. Abarbanel, Phys. Rev. E **51**, 980 (1995).
[4] M. G. Rosenblum, A. S. Pikovsky, and J. Kurths, Phys. Rev. Lett. **76**, 1804 (1996).
[5] M. G. Rosenblum, A. S. Pikovsky, and J. Kurths, Phys. Rev. Lett. **78**, 4193 (1997).
[6] T. Heil, I. Fischer, W. Elsasser, J. Mulet, and C. Mirasso, Phys. Rev. Lett. **86**, 795 (2001).
[7] J. K. White, M. Matus, and J. V. Moloney, Phys. Rev. E **65**, 036229 (2002).
[8] H. U. Voss, Phys. Rev. E **61**, 5115 (2000).
[9] H. U. Voss, Phys. Rev. Lett. **87**, 014102 (2001).
[10] C. Masoller, Phys. Rev. Lett. **86**, 2782 (2001).
[11] M. Ciszak, O. Calvo, C. Masoller, C. Mirrasso, and R. Toral, Phys. Rev. Lett. **90**, 204102 (2003).
[12] S. Sivaprakasam, E. M. Shahverdiev, P. S. Spencer, and K. A. Shore, Phys. Rev. Lett. **87**, 154101 (2001).
[13] J. Mulet, C. Mirasso, T. Heil, and I. Fischer, J. Opt. B: Quantum Semiclassical Opt. **6**, 97 (2004).
[14] L. Wu and S. Q. Zhu, Phys. Lett. A **315**, 101 (2003).
[15] A. K. Engel, P. Konig, A. K. Kreiter, and W. Singer, Science **252**, 1177 (1991).
[16] P. Konig, A. K. Engel, and W. Singer, Proc. Natl. Acad. Sci. U.S.A. **92**, 290 (1995).
[17] R. D. Traub, M. A. Whittington, I. M. Stanford, and J. G. R. Jefferys, Nature (London) **383**, 621 (1996).
[18] B. B. Zhou and R. Roy, Phys. Rev. E **75**, 026205 (2007).
[19] S. Tang *et al.*, IEEE J. Sel. Top. Quantum Electron. **10**, 936 (2004).
[20] E. Klein, N. Gross, M. Rosenbluh, W. Kinzel, L. Khaykovich, and I. Kantev, Phys. Rev. E **73**, 066214 (2006).
[21] R. Vicente, S. Tang, J. Mulet, C. R. Mirasso, and J. M. Lin, Phys. Rev. E **73**, 047201 (2006).
[22] I. Fischer, R. Vicente, J. M. Buldu, M. Peil, C. R. Mirasso, M. C. Torrent, and J. Garcia-Ojalvo, Phys. Rev. Lett. **97**, 123902 (2006).
[23] A. S. Landsman and I. B. Schwartz, Phys. Rev. E **75**, 026201 (2007).
[24] E. Rossoni, Y. Chen, M. Ding, and J. Feng, Phys. Rev. E **71**, 061904 (2005).
[25] M. Dhamala, V. K. Jirsa, and M. Ding, Phys. Rev. Lett. **92**, 074104 (2004).
[26] M. Y. Kim, R. Roy, J. L. Aron, T. W. Carr, and I. B. Schwartz, Phys. Rev. Lett. **94**, 088101 (2005).
[27] Q. L. Williams, J. Garcia-Ojalvo, and R. Roy, Phys. Rev. A **55**, 2376 (1997).
[28] L. B. Shaw, I. B. Schwartz, E. A. Rogers, and R. Roy, Chaos **16**, 015111 (2006).
[29] T. W. Carr, M. L. Taylor, and I. B. Schwartz, Physica D **213**, 152 (2006).
[30] I. B. Schwartz and T. Erneux, SIAM J. Appl. Math. **54**, 1083 (1994).
[31] L. M. Pecora and T. L. Carroll, Phys. Rev. Lett. **80**, 2109 (1998).
[32] P. Hartman, *Ordinary Differential Equations*, 2nd ed. (Birkhäuser, Boston, 1982).
[33] The intensities displayed for the fiber laser are filtered with a 125-MHz low-pass filter to correspond with a typical setup for measuring intensities experimentally [28].
[34] L. B. Shaw and I. B. Schwartz (unpublished).